Journal of Coordination Chemistry
Vol. 64, No. 22, 20 November 2011, 3859–3871

Taylor & Francis
Taylor & Francis Group

Interaction of antimony(III) chloride with thiourea, 2-mercapto-5-methyl-benzimidazole, 3-methyl-2-mercaptobenzothiazole, 2-mercaptopyrimidine, and 2-mercaptopyridine

I.I. OZTURK†‖, N. KOURKOUMELIS‡, S.K. HADJIKAKOU*†, M.J. MANOS§, A.J. TASIOPOULOS§, I.S. BUTLER¶, J. BALZARINI⊥ and N. HADJILIADIS*†

†Section of Inorganic and Analytical Chemistry, Department of Chemistry, University of Ioannina, 45110 Ioannina, Greece
‡Medical Physics Laboratory, Medical School, University of Ioannina, 45110 Ioannina, Greece
§Department of Chemistry, University of Cyprus, 1678 Nicosia, Cyprus
¶Department of Chemistry, McGill University, 801 Sherbrooke, Montreal, Quebec H2A 2K6, Canada
⊥Rega Institute for Medical Research, Katholieke Universiteit Leuven, Minderbroedersstraat 10, B-3000 Leuven, Belgium
‖Section of Inorganic Chemistry, Department of Chemistry, Namık Kemal University, 59030, Tekirdag, Turkey

(*Received 13 July 2011; in final form 29 September 2011*)

New antimony(III) chloride complexes with heterocyclic thioamides, thiourea (TU), 2-mercapto-5-methyl-benzimidazole (MMBZIM), 3-methyl-2-mercaptobenzothiazole (MMBZT), 2-mercaptopyrimidine (PMT), 2-mercaptopyridine (PYT) of formulae $[SbCl_3(TU)_2]$ (**1**), $[SbCl_3(MMBZIM)_2]$ (**2**), $[SbCl_3(MMBZT)_2]$ (**3**), $[SbCl_3(PMT)_2]$ (**4**), $[SbCl_3(\mu_2\text{-}S)(PYT)_2]$ (**5**) were synthesized and characterized by elemental analysis, FT-IR and FT-Raman spectroscopies, and TG-DTA analysis. The crystal structure of **5** was also determined by X-ray diffraction. $[C_{10}H_{10}Cl_3N_2S_2Sb]$ (**5**) crystallizes in space group $C2/c$, with $a = 25.0169(10)$ Å, $b = 9.7952(3)$ Å, $c = 12.9329(5)$ Å, $\beta = 109.702(4)^\circ$, and $Z = 8$. Crystals of **5** grown from acetonitrile solutions adopt a square-pyramidal geometry. The equatorial plane is formed by three chlorides and one sulfur atom from the thione ligand while the second sulfur is axial. The complexes were evaluated for their biological activities and compared with $[SbCl_3(MMI)_2]$ (**6**) (MMI = 2-mercapto-1-methylimidazole) and other isostructural ones. The complexes showed moderate cytostatic activity against murine leukemia cells (L1210), murine mammary carcinoma cells (FM3A), human T-lymphocyte (Molt4/C8, CEM), and human cervix carcinoma (HeLa) cells. The chloro and iodo derivatives show better cytostatic activity than the bromo ones.

Keywords: Bioinorganic chemistry; Antimony(III) chloride complexes; Thioamides; Crystal structure; Cytotoxic activity

*Corresponding authors. Email: shadjika@uoi.gr; nhadjis@uoi.gr

ISSN 0095-8972 print/ISSN 1029-0389 online
http://dx.doi.org/10.1080/00958972.2011.633603

1. Introduction

Antimony has been used as a drug for over 100 years. The major clinical use of antimony compounds is as treatment for Leishmaniasis [1, 2]. However, antitumor activities of some antimony compounds were reported during the mid-1960s [3, 4]. The antitumor screening and cytotoxicity of antimony(III) and antimony(V) compounds have also been reviewed by Tiekink [5]. The most studied antimony(III) compounds, in the context of antitumor activity, are organoantimony compounds, such as diphenylantimony(III) thiolates, i.e., $[Ph_2Sb(S_2PPh_2)]$ and $[Ph_2Sb(S_2P(O^iPr)_2)]$ [6–8]. Early studies of these compounds showed that either *in vitro* or *in vivo* they were more active than the corresponding organotin(IV) compounds against Ehrlich ascites tumor cell lines [6–8]. Hsu *et al.* [3, 4] demonstrated that antimony(III) compounds with aminopolycarboxy ligands increased the life span of mice bearing the Ehrlich ascites tumor and spindle sarcoma. Other reports showed that some tungstoantimonates with complicated compositions also exhibited antitumor activity [9, 10]. Antimony (s-benzyldithiocarbazate) complexes display antitumor agents against melanoma (skin cancer cells) [11].

We have recently shown that antimony(III) chloride, bromide, or iodide complexes with sulfur donors such as thioamides also exhibit antitumor properties [12–14]. Complexes were tested *in vitro* for their inhibitory effect on proliferation of murine leukemia cells (L1210), murine mammary carcinoma cells (FM3A), human T-lymphocyte cells (Molt4/C8, CEM), and human cervix carcinoma cells (HeLa). Surprisingly, antimony(III) thione complexes consistently showed selective antiproliferative activity against HeLa cells.

In this article, we report the synthesis and spectroscopic characterization of five new antimony(III) chloride complexes with heterocyclic thioamides (scheme 1), thiourea (TU), 2-mercapto-5-methyl-benzimidazole (MMBZIM), 3-methyl-2-mercaptobenzothiazole (MMBZT), 2-mercaptopyrimidine (PMT), 2-mercaptopyridine (PYT) of formulae $[SbCl_3(TU)_2]$ (**1**), $[SbCl_3(MMBZIM)_2]$ (**2**), $[SbCl_3(MMBZT)_2]$ (**3**),

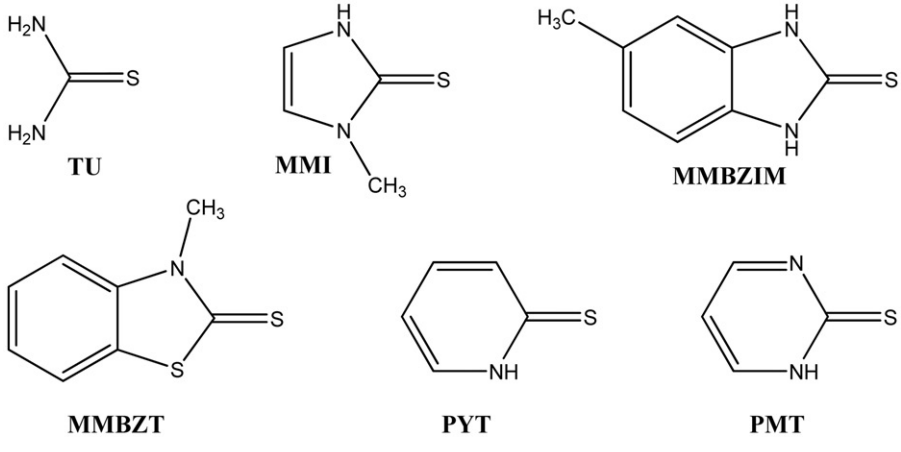

Scheme 1. Formulae of the ligands used.

$[SbCl_3(PMT)_2]$ (**4**), and $[SbCl_3(\mu_2\text{-S})(PYT)_2]$ (**5**). The X-ray crystal structure of **5** is also reported. The known compound $[SbCl_3(MMI)_2]$ (**6**) (MMI = 2 mercapto-1-methylimidazole) [15] was also evaluated for its antitumor properties and compared with those of **1**–**5**.

2. Results and discussion

2.1. *General aspects*

Antimony(III) chloride complexes **1**–**6** have been synthesized by reacting the appropriate thione with an excess of antimony(III) chloride ($SbCl_3$) in methanolic/acetonitrile or dichloromethane solutions as shown by equations (1) and (2). The ligands are coordinated to Sb(III) through their neutral forms and no deprotonation occurs.

All complexes are formed as air-stable powders. Crystals of **5** suitable for X-ray analysis were grown from acetonitrile solutions.

$$SbCl_3 + 2HL \xrightarrow[\text{(b) } CH_3CN, CH_3OH]{\text{(a) } CH_2Cl_2,\ \text{re-cryst.}CH_3CN} Sb(HL)_2Cl_3 \qquad (1)$$

(a) HL = MMBZIM, MMBZT

(b) HL = TU, MMI, PMT

$$2SbCl_3 + 4PYT \xrightarrow{\text{(a) } CH_2Cl_2,\ \text{re-cryst.}CH_3CN} \left[SbCl_3(\mu_2\text{-S})(PYT)_2\right]_2 \qquad (2)$$

2.2. *Thermal analysis*

TG-DTA analysis of **1**–**6** (under N_2) was carried out from 30°C to 850°C (figures S1–S6). The TG and DTA diagrams of **1**, **3**, **4**, **5** and **6** (figures S1, S3–S6), which adopt square-pyramidal (SP) geometries around Sb(III) (see section 2.3), showed one decomposition step (119–500°C (**1**), 132–246°C (**3**), 70–745°C (**4**), 90–300°C (**5**), and 73–670°C (**6**)), corresponding to evolution of two thione ligands and three chlorides 64.4% **1**, 84.27% **3**, 72.9% **4**, 73.1% **5**, 65.9% **6** (calculated mass loss 64.9% (**1**), 80% (**3**), 73.1% (**4**), 73% (**5**) 73% (**6**)) (reaction 3).

Thermal analysis of **2**, which also has SP geometry around Sb(III), (see section 2.3), shows two step decomposition (figure S2). The first stage (60–452°C) involves 64% mass loss, corresponding to evolution of two MMBZIM ligands and one chloride (calculated mass loss 65%) (reaction 4). The second stage of decomposition (452–658°C) corresponds to 11.4% mass loss of two chlorides (calculated mass loss 12.7%) (reaction 4).

$$\underset{1,3,4,5,6}{\left[Sb(HL)_2Cl_3\right]_n} \xrightarrow{-2nHL,\ -3nCl} nSb \qquad (3)$$

$$\underset{2}{\left[Sb(HL)_2Cl_3\right]_n} \xrightarrow{-2nHL,\ -nCl} [SbCl]_n \xrightarrow{-nCl} nSb \qquad (4)$$

2.3. *Vibrational spectroscopy*

IR spectra of the complexes show distinct vibrational bands at 1578–1389 cm^{-1} and 1377–1261 cm^{-1}, which can be assigned to ν(CN) (thioamide I and II bands) and at 1168–972 cm^{-1} and 744–637 cm^{-1}, which are attributed to ν(CS) (thioamide III and thioamide IV bands) [16–18].

Far-IR spectra of **1**–**6** show distinct vibrational bands between 279 and 340 cm^{-1}, which are assigned to ν(Sb–Cl) [12]. The ν(Sb-S) vibration bands are between 234 and 273 cm^{-1} [12, 19]. Thus, in $SbCl_3(PYT)_2$ (**5**), bands at 270 and 258 cm^{-1} are assigned to the $\nu(Sb–S_{(terminal)})$ and $\nu(Sb\text{-}S_{(bridging)})$ vibrations, respectively, whereas ν(Sb–Cl) appears at 312 cm^{-1}. For **1**–**4** and **6**, where no structural data are available, far-IR spectra can be used for assignment of geometry. Thus, far-IR spectra of **1** and **3** show one ν(Sb–Cl) band at 279 (**1**) or 305 (**3**) cm^{-1} and one ν(Sb–S) band at 249 (**1**) or 234 (**3**) cm^{-1}, both assigned to terminal Sb–Cl and Sb–S stretching bands which classify them as monomers [12–14] (scheme 2a). Far-IR spectra of **2** and **4** show bands at 340 and 328 cm^{-1} (**2**) and 335 and 314 cm^{-1} (**4**) for ν(Sb–Cl) terminal and bridging vibrations and a band at 280 (**2**) and 271 (**4**) cm^{-1} for terminal ν(Sb–S). These data classify **2** and **4** as dimers or polymers with chloride bridges [12–14] (scheme 2b). For **6**, however, far-IR spectrum shows bands at 338 cm^{-1} for ν(Sb–Cl) vibrations and at 273 and 256 cm^{-1} for terminal and bridging ν(Sb-S) vibrations, indicating either dimer or polymer with sulfur bridges [12–14] (scheme 2c).

The Raman spectra of **1**–**6** show vibrational bands from 304 to 339 cm^{-1} and 276 to 279 cm^{-1} assigned to $\nu(Sb–Cl_{(terminal)})$ and $\nu(Sb–Cl_{(bridging)})$, respectively. Bands between 224–258 cm^{-1} and 200–201 cm^{-1} are assigned to $\nu(Sb–S_{(terminal)})$ and $(Sb–S_{(bridging)})$ vibrations, respectively [12, 20, 21]. Raman spectra of **1** and **3** show one ν(Sb–Cl) band at 304 (**1**) or 330 cm^{-1} (**3**) and one ν(Sb–S) band at 234 cm^{-1} (**1**) or 224 cm^{-1} (**3**), which classify them as monomers with *cis*-S and *cis*-Cl arrangements [22] (scheme 2a). Complexes **5** and **6** with one bridging and one terminal sulfur exhibit $\nu(Sb–S_{(terminal)})$ bands at 257 cm^{-1} (**5**) and 258 cm^{-1} (**6**), $\nu(Sb–S_{(bridging)})$ bands at 201 cm^{-1} (**5**) and 200 cm^{-1} (**6**) with ν(Sb–Cl) bands at 316 cm^{-1} (**5**) and 304 cm^{-1} (**6**), which classify them as dimeric with b,c,d-Cl arrangement [15] (scheme 2c). Complexes **2** and **4** with one bridging and one terminal chloride exhibit $\nu(Sb–Cl_{(terminal)})$ bands at 327 cm^{-1} for **2** or 327 cm^{-1} for **4** and $\nu(Sb–Cl_{(bridging)})$ bands at 276 cm^{-1} (**2**) or 279 cm^{-1} (**4**); ν(Sb–S) bands appear at 234 cm^{-1} (**2**) and 227 cm^{-1} (**4**), classifying **2** as dimer with *trans*-S and *trans*-Cl arrangements (scheme 2b) and **4** as either dimer or polymer with b,c,d-Cl arrangement (scheme 2b).

2.4. *Crystal and molecular structure of [$SbCl_3(PYT)_2$]*

Crystal structures of antimony(III) chloride-thione compounds are rare [12, 15, 23]. The geometries: adopted by these complexes are either: (i) octahedral (Oh); (ii) SP with either *cis*-Cl, *cis*-S arrangement, *trans*-Cl, *trans*-S arrangement or *b*,*c*,*d*-Cl arrangement, and (iii) pseudotrigonal bipyramidal (ψ-TBP) geometries (scheme 2). For monomers of SP geometry secondary Sb···Cl or/and Sb···S interactions lead to dimeric or polymeric chains.

ORTEP diagram of **5** as well as selected bond lengths and angles are shown in figure 1. The antimony(III) chloride compound **5** is dimeric, built from monomeric units with SP geometries around antimony. Two sulfur donors from thioamide and

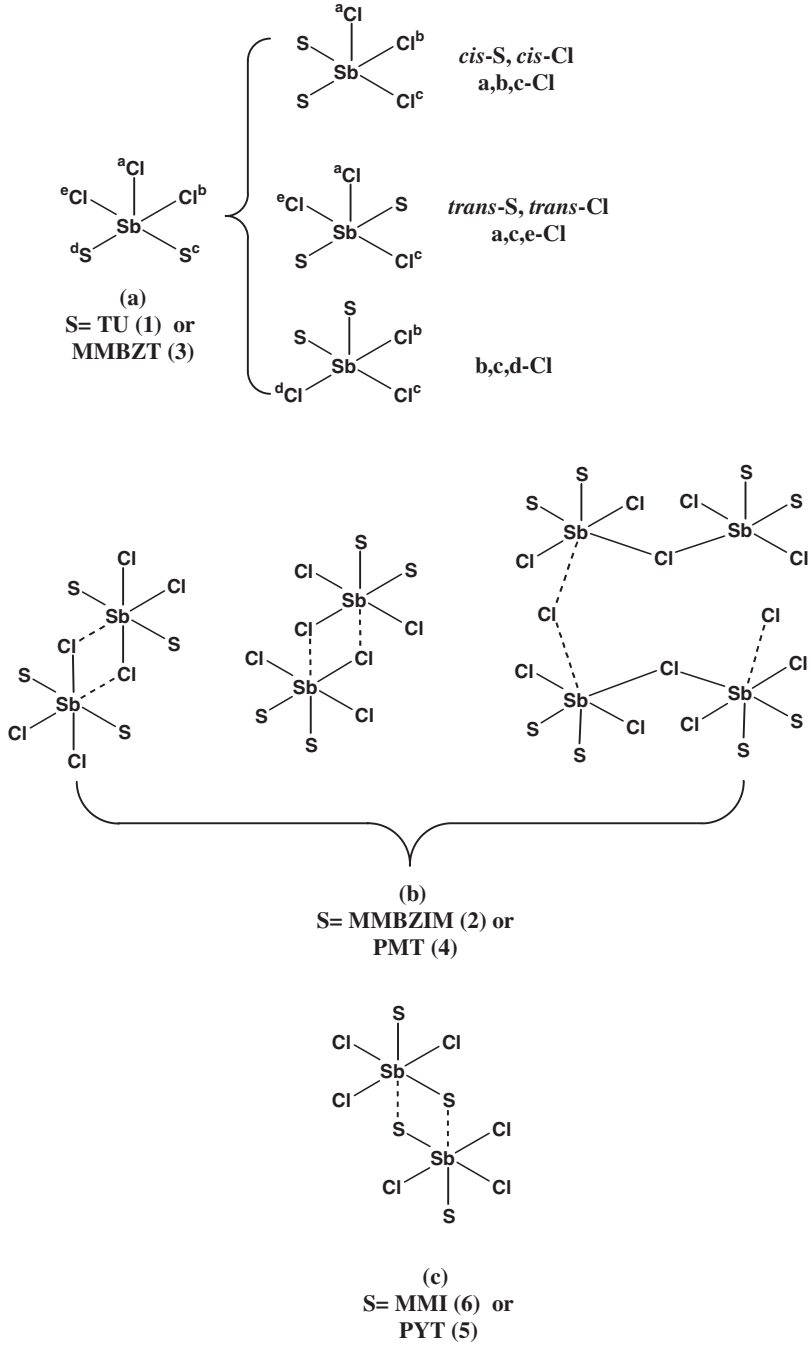

Scheme 2. Geometries adopted by antimony(III) trichloride complexes.

three chlorides are bonded to Sb forming the building blocks of the dimer. Strong intramolecular interactions between μ_2-S and Sb (Sb1–S1a = 3.296 Å) lead to a dimeric assembly with pseudooctahedral (ψ-Oh) geometry around Sb(III). The sum of van der Waals radii for the Sb–S bond is 4.0–4.47 Å [24].

The Sb–S bond distances are Sb1–S1 = 2.7724(9) and Sb1–S2 = 2.5227(10) Å, respectively (figure 1). These distances are in the range of corresponding Sb–S distances varying from 2.482 to 2.849 Å found in $\{[SbCl_2(MBZIM)_4]^+Cl^- \cdot 2H_2O \cdot (CH_3OH)\}$ [12], $\{[SbCl_2(MBZIM)_4]^+Cl^- \cdot 3H_2O \cdot (CH_3CN)\}$ [12], a,b,c-Cl-[$SbCl_3(MBZIM)_2$] [12], a,b,d-Cl-[$SbCl_3(EtMBZIM)_2$] [12], a,b,c-Cl-[$SbCl_3(MTZD)_2$] [12], and b,c,d-Cl-[$SbCl_3(tHPMT)_2$] [12] complexes.

The Sb–Cl bond distances lie between 2.4938(9) and 2.7484(10) Å (figure 1) (van der Waals radii for Sb-Cl bonds is 3.95 Å [25]). These bond distances are similar to those found in $\{[SbCl_2(MBZIM)_4]^+Cl^- \cdot 2H_2O \cdot (CH_3OH)\}$ [12], $\{[SbCl_2(MBZIM)_4]^+Cl^- \cdot 3H_2O \cdot (CH_3CN)\}$ [12], a,b,c-Cl-[$SbCl_3(MBZIM)_2$] [12], a,b,d-Cl-[$SbCl_3(EtMBZIM)_2$] [12], a,b,c-Cl-[$SbCl_3(MTZD)_2$] [12], and b,c,d-Cl-[$SbCl_3(tHPMT)_2$] [12], where Sb–Cl bond lengths lie between 2.376 and 3.010 Å.

The C–S bond distances are 1.735(3) and 1.756(4) Å in **5**, supporting ligand coordination through thionate form (average C–S = 1.69–1.72 Å) [26–28]. The basal bond angles deviate from ideal values of 180° or 90° (Cl1–Sb1–Cl2 = 85.80(3)° and Cl1–Sb–Cl3 = 170.72(3)°). This is due to valence shell electron pair repulsion between the lone pair of electrons located on Sb and those of the basal bonds [29].

2.5. *Computational studies*

Since multiple secondary bonding interactions stabilize the packing in the solid state, we performed a computational study on the electronic properties of the structure derived by crystallographic techniques. In figure 2(a) and (b), highest occupied molecular orbital (HOMO) and the lowest unoccupied molecular orbital (LUMO) are depicted. The contribution of Sb to the HOMO is negligible while the presence of the lone pair is far more obvious in HOMO–3 (figure 2c). The lone pair has more *p* orbital character, therefore realizing itself in the coordination sphere triggering a distortion from the ideal symmetrical structure. The stereochemically active role of the lone pair is evident in the packing diagram of the crystal structure as discussed earlier [18].

APT atomic charge distribution shows that Cl^- which does not participate in bond formation with adjacent asymmetric units is less basic (APT charge = −0.32e) than the other two chlorides (APT charge = −0.44, −0.37e). It is therefore concluded that the crystallographic long chain during complex formation increases negative charge, weakening the Sb–Cl bonds.

2.6. *Cell screening*

Complexes **1**–**6** were tested *in vitro* for their inhibitory effects on proliferation of murine leukemia cells (L1210), murine mammary carcinoma cells (FM3A), human T-lymphocyte cells (Molt4/C8, CEM), and human cervix carcinoma cells (HeLa). The results of this study are reported as 50% inhibitory concentration (IC_{50}) values in table 1. Complexes **1**–**6** show modest cytostatic activity against the tumor cell lines studied (table 1). Antimony trichloride complexes tested here consistently show selective

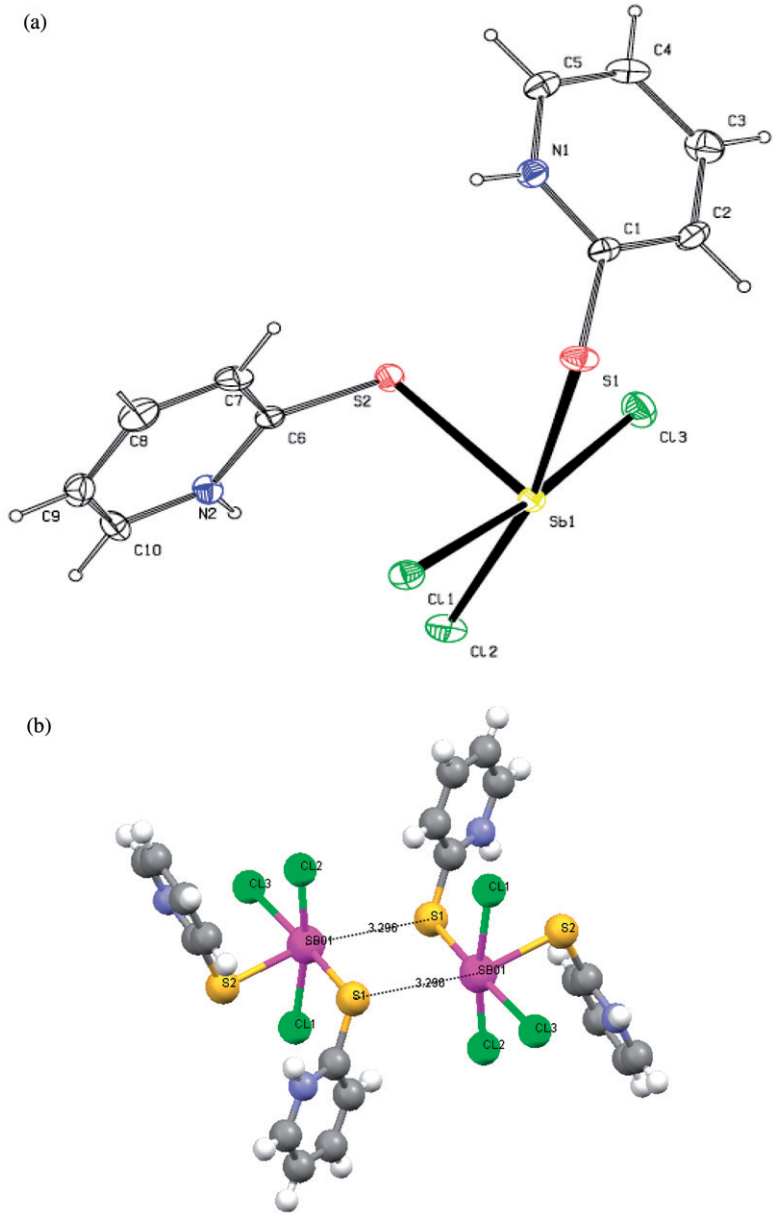

Figure 1. (a) ORTEP diagram of *b*,*c*,*d*-Cl-[$SbCl_3(PYT)_2$] (**5**) together with the atomic numbering scheme. Thermal ellipsoids drawn at the 50% probability level. (b) Two μ_2-S$\cdots$Sb and one μ_2-S$\cdots$Sb, intramolecular interactions, finally lead to dimerization with ψ-Oh geometry around Sb center. Selected bond lengths (Å) and angles (°). 2.4938(9), Sb1–Cl2 = 2.6102(9), Sb1–Cl3 = 2.7484(10), Sb1–S1 = 2.7724(9), Sb1–S2 = 2.5227(10), S1–C1 = 1.735(3), S2–C6 = 1.756(4), Sb1$\cdots$S1a = 3.296, Cl1–Sb1–Cl2 = 85.80(3), Cl1–Sb1–Cl3 = 170.72(3), Cl1–Sb1–S1 = 85.61(3), Cl1–Sb1–S2 = 94.55(3), Cl2–Sb1–Cl3 = 89.40(3), Cl2–Sb1–S1 = 168.52(3), Cl2–Sb1–S2 = 86.68(3) Cl3–Sb1–S1 = 98.01(3), Cl3–Sb1–S2 = 77.22(3), S1–Sb1–S2 = 86.43(3), Sb1–S1$\cdots$Sba = 109.25, S1a$\cdots$Sb1–S1 = 70.75.

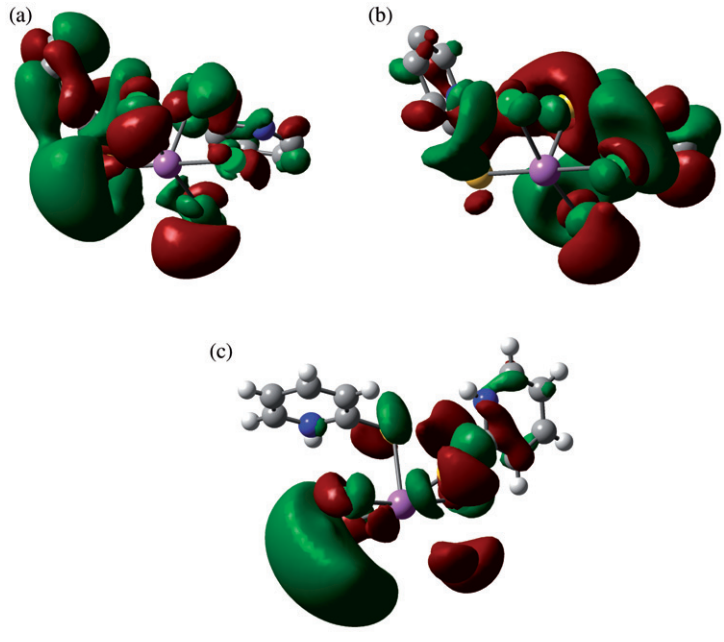

Figure 2. (a) HOMO, (b) LUMO, and (c) HOMO-3 molecular orbitals.

Table 1. Cytostatic activity of the compounds against murine leukemia Cells (L1210), murine mammary carcinoma cells (FM3A), human T-lymphocyte (Molt4/C8, CEM), and human cervix carcinoma (HeLa) cells.

	IC_{50}[a] ($\mu g\,mL^{-1}$)					
Sb(III) halide compounds	L1210	FM3A	Molt4/C8	CEM	Hela	Ref.
$[SbCl_3(TU)_2]$ (**1**)	19.1	56.2	20.0	48.0	3.9	This study
$[SbCl_3(MMI)_2]$ (**6**)	19.5	24.2	21.4	38.9	2.9	This study
$[SbCl_3(MMBZIM)_2]$ (**2**)	38.5	28.2	26.9	43.6	3.3	This study
$[SbCl_3(MMBZT)_2]$ (**3**)	24.2	74.4	25.4	24.8	7.1	This study
$[SbCl_3(PMT)_2]$ (**4**)	8.0	27.7	9.4	23.5	1.4	This study
$[SbCl_3(\mu_2\text{-S})(PYT)_2]$ (**5**)	19.4	63.9	11.2	24.8	0.9	This study
Cisplatin	0.07		0.1		3.00	[13]
Carboplatin					>11.1	[13]
$[SbBr_3(TU)_2]$	20	47	12	55	12	[13]
$[SbBr_3(MMI)_2]$	42	72	27	75	17	[13]
$[SbBr_3(MMBZIM)_2]$	24	52	14	50	14	[13]
$[SbBr_3(MMBZT)_2]$	43	57	15	31	16	[13]
$[SbBr_3(PMT)_2]$	15	37	9.4	44	3.1	[13]
$[SbBr_3(PYT)_2]$	19	56	13	42	3.7	[13]
$\{[SbI_3(MMI)_2]\cdot MeOH\}$	72	136	44	101	21	[14]
$[(MMBZT)SbI_2(\mu_2\text{-I})_2(\mu_2\text{-MMBZT})$ $SbI_2(MMBZT)]$	28	63	15	34	5	[14]
$[SbI_3(PMT)_2]$	28	76	23	33	3	[14]
$[SbI_3(PYT)]$	22	55	16	36	3	[14]

[a]50% inhibitory concentration.

Table 2. Antimony(III) trichloride complexes activities against HeLa cells and their structural data.

Compound	d(C=S)[a]	HeLa ($\mu g\,mL^{-1}$)	Ref.
$[SbCl_3(PYT)_2]$ (a)	1.7455	0.9	This study
$[SbCl_2(MBZIM)_4]^+Cl^- \cdot 2H_2O \cdot CH_3OH$ (b)	1.7098	5.7	[12]
$[SbCl_2(MBZIM)_4]^+Cl^- \cdot 3H_2O \cdot CH_3CN$ (c)	1.698	6.1	[12]
$[SbCl_3(MBZIM)_2]$ (d)	1.704	4.1	[12]
$[SbCl_3(EtMBZIM)_2]$ (e)	1.7115	4.3	[12]
$[SbCl_3(MTZD)_2]$ (f)	1.7205	3.2	[12]
$[SbCl_3(tHPMT)_2]$ (g)	1.7541	3.5	[12]

[a]Average bond length.

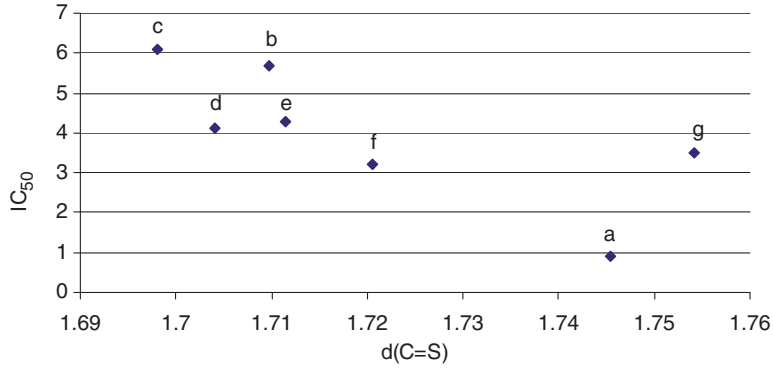

Figure 3. Correlation plot of cytostatic activity (IC_{50}) of antimony(III) trichloride compounds against human cervix carcinoma (HeLa) cells and C=S average bond distances (Å) (a) $[SbCl_3(PYT)_2]$, (b) $\{[SbCl_2(MBZIM)_4]^+Cl^-2H_2O$ $(CH_3OH)\}$, (c)$\{[SbCl_2(MBZIM)_4]^+Cl^-3H_2O$ $(CH_3CN)\}$, (d) $[SbCl_3(MBZIM)_2]$, (e) $[SbCl_3(EtMBZIM)_2]$, (f) $[SbCl_3(MTZD)_2]$, and (g) $[SbCl_3(tHPMT)_2]$.

cytotoxic activities against HeLa cells, also observed when antimony tri-halide complexes of thioamides were evaluated for their cytotoxicity previously [12–14]. Among complexes **1**–**6** tested, $[SbCl_3(\mu_2\text{-}S)(PYT)_2]$ (**5**) exhibits the strongest activity against HeLa cells with IC_{50} value of 0.9 (**5**) $\mu g\,mL^{-1}$ (table 1). Antimony(III) bromide or iodide complexes of PYT were also evaluated for their activity against HeLa cells $\{SbBr_2(\mu_2\text{-}Br)(PYT)_2)_n\}$ ($IC_{50} = 3.7\,\mu g\,mL^{-1}$) [13], $[SbI_3(PYT)]$ ($IC_{50} = 3.8\,\mu g\,mL^{-1}$) [14] and they were less active than **5** (table 1). Finally, **5** shows three times higher activity than cisplatin and 11 times higher than carboplatin against HeLa cells.

The cell screening results of other antimony(III) trichloride complexes, of which crystallographic data are available, are shown in table 2. Among them **5** shows the strongest activity against HeLa cells (table 2). Moreover, a correlation plot between cytostatic activity of the compounds against human cervix carcinoma (HeLa) cells (IC_{50}) and C=S average bond distances (Å) of antimony chloride complexes tested to date show that longer C=S bond (stronger Sb–S interaction) leads to stronger activity (figure 3) which may imply the involvement of the whole molecule in the antitumor action, without S–Sb bond cleavage.

3. Conclusions

Complexes **1**–**6** show moderate cytostatic activity against murine leukemia cells (L1210), Murine mammary carcinoma cells (FM3A), human T-lymphocyte (Molt4/C8, CEM), and human cervix carcinoma (HeLa) Cells. Antimony(III) trichloride complexes tested here consistently showed selective cytotoxic activities against HeLa cells higher than those of cisplatin and carboplatin (table 1), which was also observed when antimony tri-halide complexes of thioamides were evaluated for their cytotoxicity previously [12–14]. Among antimony(III) trichloride complexes tested to date, **5** shows the strongest activity against HeLa cells (table 2). The C=S average bond distances of the compounds tested against HeLa cells correlate with their cytostatic activity.

4. Experimental

4.1. *Materials and instruments*

All solvents used were of reagent grade. Antimony(III) chloride (Fluka) as well as thiones thiourea, 2-mercapto-5-methylbenzimidazole, 3-methyl-2-benzothiazolinthion, 2-mercaptopyrimidine (Aldrich), 2-mercaptopyridine (Fluka), and 2-mercapto-1-methylimidazole (Sigma) were used without purification. Elemental analyses for C, H, N, and S were carried out with a Carlo Erba EA MODEL 1108 elemental analyzer. Melting points were measured in open tubes with a STUART scientific apparatus and are uncorrected. UV-Vis spectra were collected in a UV-Vis/NIR V570 instrument. IR spectra from 4000 to 370 cm^{-1} were obtained for KBr pellets, whereas far-IR spectra (400–50 cm^{-1}) were measured for polyethylene discs with a Perkin Elmer Spectrum GX FTIR spectrometer. Micro Raman spectra (64 scans) were recorded at room temperature using a low-power (~30 mW) green (514.5) mm laser on a Renishaw In Via spectrometer set at 2.0 resolution. Thermal studies were carried out on a Shimadzu DTG-60 simultaneous DTA-TG apparatus under N_2 flow (50 $cm^3\,min^{-1}$) at a heating rate of 10°C min^{-1}.

4.2. *Synthesis and crystallization of $[SbCl_3(TU)_2]$ (1), $[SbCl_3(MMBZIM)_2]$ (2), $[SbCl_3(MMBZT)_2]$ (3), $[SbCl_3(PMT)_2]$ (4), $[SbCl_2(\mu_2\text{-}S)(PYT)_2]_2$ (5), and $[SbCl_3(MMI)_2]$ (6)*

1.0 mmol of the thioamides, 5-methyl-2-mercaptobenzimidazole (0.164 g), 3-methyl-2-mercaptobenzothiazole (0.181 g), and 2-mercaptopyridine (0.111 g) were dissolved in 10 cm^3 dichloromethane, while 1 mmol of thiourea (0.076 g), 2-mercapto-1-methylimidazole (0.114 g), and 2-mercaptopyrimidine (0.112 g), were dissolved in acetonitrile (10 cm^3). A solution of antimony(III) chloride (0.114 g, 5.0 mmol) in dichloromethane (10 cm^3) for **3**, **4**, and **6** or in methanol (10 cm^3) for **1**, **2**, and **5** was then added to the above solution. The solution of **1**, **2**, and **5** was filtered off, and the resulting clear solutions were kept in the dark at room temperature to form powders of the complexes upon slow evaporation. For **3**, **4**, and **6**, the solutions were stirred for 30 min and the resulting precipitates were filtered off and dried. Re-crystallization of the solid powder

with hot acetonitrile (20 cm^3) yields crystals of **5**. All solid products are stable when kept in darkness at room temperature.

1: yellow powder; yield, 75%; mw, 380.36 g mol^{-1}. Elemental analyses, found: C, 6.35; H, 2.20; N, 14.60; S, 16.73. Anal. Calcd for $C_2H_8Cl_3N_4S_2Sb$: C, 6.32; H, 2.12; N, 14.73; S, 16.86. IR (cm^{-1}): 3282s, 3188s, 1636s, 1420m, 1389m, 1055w, 707m, 577m, 472m.

2: green powder; yield, 82%; mw, 556.57 g mol^{-1}. Elemental analyses, found: C, 34.12; H, 2.83; N, 9.95; S, 11.38. Anal. Calcd for $C_{16}H_{16}Cl_3N_4S_2Sb$: C, 34.53; H, 2.90; N, 10.07; S, 11.52. IR (cm^{-1}): 3111s, 1617m, 1518w, 1491s, 1461s, 1388w, 1350w, 1326m, 1260w, 1229w, 1179m, 1134w, 983w, 861w, 799s, 709m, 626m, 593m, 540m, 478w, 429w, 385w.

3: yellow powder; yield, 85%; mw, 590.67 g mol^{-1}. Elemental analyses, found: C, 32.89; H, 2.43; N, 4.77; S, 21.84. Anal. Calcd for $C_{16}H_{14}Cl_3N_2S_4Sb$: C, 32.53; H, 2.39; N, 4.74; S, 21.71. IR (cm^{-1}): 3434m, 1581w, 1460m, 1428m, 1366s, 1319m, 1268w, 1134m, 1096s, 1054m, 974s, 753s, 717w, 637w, 536m, 425w.

4: yellow powder; yield, 80%; mw, 452.42 g mol^{-1}. Elemental analyses, found: C, 21.15; H, 1.83; N, 12.31; S, 14.03. Anal. Calcd for $C_8H_8Cl_3N_4S_2Sb$: C, 21.24; H, 1.78; N, 12.38; S, 14.17. IR (cm^{-1}): 3386m, 1555s, 1427w, 1377s, 1195m, 1168m, 986w, 798w, 767w, 744m, 629w, 469w.

5: yellow crystal; yield, 85%; mw, 450.45 g mol^{-1}. Elemental analyses, found: C, 26.73; H, 2.14; N, 6.35; S, 14.32. Anal. Calcd. for $C_{10}H_{10}Cl_3N_2S_2Sb$: C, 26.66; H, 2.24; N, 6.22; S, 14.24. IR (cm^{-1}): 3449m, 1603m, 1578s, 1509m, 1442m, 1421w, 1366w, 1261m, 1160w, 1128s, 1082w, 1036w, 998w, 752s, 724m, 620w, 485w, 438w.

6: yellow powder; yield, 80%; mw, 456.46 g mol^{-1}. Elemental analyses, found: C, 20.94; H, 2.70; N, 12.26; S, 13.85. Anal. Calcd for $C_8H_{12}Cl_3N_4S_2Sb$: C, 21.05; H, 2.65; N, 12.27; S, 14.05. IR (cm^{-1}): 3435s, 1627w, 1571s, 1461m, 1443m, 1283m, 1155m, 1095m, 918w, 740s, 671s, 511w, 405w.

4.3. *X-ray structure determination*

Intensity data for crystals of **5** were collected on an Oxford Diffraction CCD instrument [30] using graphite-monochromated Mo radiation ($\lambda = 0.71073$ Å). Cell parameters were determined by least-squares refinement of the diffraction data from 25 reflections [31].

All data were corrected for Lorentz-polarization effects and absorption [30, 31]. The structure was solved with direct methods with SHELXS-97 [32] and refined by full-matrix least-squares on F^2 with SHELXL-97 [33]. All non-hydrogen atoms were refined anisotropically, hydrogen atoms were located at calculated positions and refined *via* the "riding model" with isotropic thermal parameters fixed at 1.2 (1.3 for CH_3 groups) times the U_{eq} value of the appropriate carrier atom.

5: $C_{10}H_{10}Cl_3N_2S_2Sb$: MW = 450.45, Monoclinic, space group $C2/c$, $a = 25.0169(10)$, $b = 9.7952(3)$, $c = 12.9329(5)$ Å, $\beta = 109.702(4)^\circ$, $V = 2983.6(2)$ $Å^3$, $Z = 8$, $T = 100$, $\rho(\text{Calcd}) = 2.006$ g cm^{-3}, $\mu = 2.6$ mm^{-1}, $F(000) = 1744$. Total reflections measured 5995, unique reflections (R(int)) 3093 (0.036). The refinement converged to final R [for 2623 reflections with $I > 2\sigma(I)$] = 0.0300. $wR = 0.0674$ ($S = 1.00$).

4.4. *Computational studies*

All calculations were carried out using the GAUSSIAN-03W software package [34] and the results were obtained by employing density functional method (DFT) by utilizing Becke's three-parameter fit of the exact exchange correlation potential [35] in combination with the gradient-corrected functional of Lee *et al*. [36], (B3LYP). Single point calculations were done with the LanL2DZ double-zeta effective core potential basis set to describe the valence electrons of Sb and with the standard basis set 6-31G (d,p) for all other atoms.

4.5. *Cytostatic activity assays*

Murine leukemia L1210, murine mammary carcinoma FM3A, human T-lymphocyte Molt 4 and CEM, and human cervix carcinoma HeLa cells were suspended at 300,000–500,000 cells per mL in a culture medium, and 100 μL of a cell suspension was added to 100 μL of an appropriate dilution of the test compounds in a 96-well microtiter plate apparatus. After incubation at 37°C for two (L1210 and FM3A) or three (Molt4, CEM and HeLa) days, the cell number was determined using a Coulter counter. The number of the suspension cells was counted directly; the number of the monolayer HeLa cells was counted after detachment of the cells upon trypsinization. The IC_{50} level was defined as the compound concentration required to inhibit cell proliferation by 50%.

Supplementary material

Supplementary data are available from the CCDC, 12 Union Road, Cambridge CB2 1EZ, U.K. (E-mail: deposit@ccdc.cam.ac.uk), on request, quoting deposition no. CCDC-825901 for **5**.

Acknowledgments

This research was carried out in partial fulfillment of the requirements for the PhD thesis of I.I.O., under the supervision of S.K.H., under the framework of the graduate program in Bioinorganic Chemistry, coordinated by N.H., at the University of Ioannina. S.K.H., N.H., and I.S.B. would like to acknowledge a NATO grant for the exchange of scientists (PDD(CP)-(CBP.NR.NRCLG 983167). I.I.O. thanks the Hellenic Ministry of Education for a scholarship for postgraduate studies.

References

[1] J.W. Tracy, L.T. Webster. *The Pharmacological Basis of Therapeutics*, 9th Edn, pp. 987–1008, McGraw-Hill, New York (1995).
[2] D.J. Berman. *Rev. Infect. Dis*., **10**, 560 (1988).

[3] B. Hsu, C.H. Chou, J.T. Chen, M.L. Shen. *Chin. Med. J.*, **82**, 155 (1963).
[4] B. Hsu, C.H. Chou, J.T. Chen, M.L. Shen. *Acta Unio Intern. Contra Cancrum*, **20**, 245 (1964).
[5] E.R.T. Tiekink. *Crit. Rev. Oncol./Hematol.*, **42**, 217 (2002).
[6] C. Silvestru, C. Socaciu, A. Bara, L. Haiduc. *Anticancer Res.*, **10**, 803 (1990).
[7] A. Bara, C. Socaciu, C. Silvestru, I. Haiduc. *Anticancer Res.*, **11**, 1651 (1991).
[8] C. Socaciu, A. Bara, C. Silvestru, I. Haiduc. *In Vivo*, **5**, 425 (1991).
[9] C. Jasmin, J-C. Chermann, G. Herve, A. Teze, P. Souchay, C. Boyloust, N. Raybaud, F. Sinoussi, M. Raynaud. *J. Natl. Cancer Inst.*, **53**, 469 (1974).
[10] R. Lidereau, C. Bouchet, F. Sinoussi, R. Saracino, J.C. Cherman. *Curr. Chemother. Proc.*, **2**, 1323 (1978).
[11] E. Hounghn, D.G. Nicholsan. *J. Chem. Soc., Dalton Trans.*, 2083 (1981).
[12] I.I. Ozturk, S.K. Hadjikakou, N. Hadjiliadis, N. Kourkoumelis, M. Kubicki, M. Baril, I.S. Butler, J. Balzarini. *Inorg. Chem.*, **46**, 8652 (2007).
[13] I.I. Ozturk, S.K. Hadjikaou, N. Hadjiliadis, N. Kourkoumelis, M. Kubicki, A.J. Tasiopoulos, H. Scleiman, M.M. Barsan, I.S. Butler, J. Balzarini. *Inorg. Chem.*, **48**, 2233 (2009).
[14] I.I. Ozturk, S. Filimonova, S.K. Hadjikakou, N. Kourkoumelis, V. Dokorou, M.J. Manos, A.J. Tasiopoulos, M.M. Barsan, I.S. Butler, E.R. Milaeva, J. Balzarini, N. Hadjiliadis. *Inorg. Chem.*, **49**, 488 (2010).
[15] P. Berges, W. Hinrichs, J. Kopf, D. Mandak, G. Klar. *J. Chem. Res.*, **218**, 2601 (1985).
[16] V. Daga, S.K. Hadjikakou, N. Hadjiliadis, M. Kubicki, J.H.Z. dos Santos, I.S. Butler. *Eur. J. Inorg. Chem.*, 1718 (2002).
[17] P.C. Zachariadis, S.K. Hadjikakou, N. Hadjiliadis, A. Michaelidis, S. Skoulika, J. Balzarini, S. De Clercq. *Eur. J. Inorg. Chem.*, 1420 (2004).
[18] S.K. Hadjikakou, C.D. Antoniadis, N. Hadjiliadis, M. Kubicki, J. Binolis, S. Karkabounas, K. Charalabopoulos. *Inorg. Chim. Acta*, **358**, 2861 (2005).
[19] M.G.B. Drew, J.M. Kisenyi, G.R. Willey, S.O. Wandiga. *J. Chem. Soc., Dalton Trans.*, 1717 (1984).
[20] C. Ludwig, M. Dolny, H.-J. Gotze. *Spectrochim. Acta, Part A*, **56**, 547 (2000).
[21] T.M. Klapotke, H. Noth, T. Schutt, M. Warchold. *Z. Anorg. Allg. Chem.*, **627**, 81 (2001).
[22] K.M. Upadhya, N.K. Udayashankar. *Synth. React. Inorg. Met.-Org., Nano-Met. Chem.*, **40**, 812 (2010).
[23] (a) E. Hough, D.G. Nicholson. *J. Chem. Soc., Dalton Trans.*, 2083 (1981); (b) B. Rubin, F.J. Heldrich, W.K. Dean, D.J. Williams, A. Viehbeck. *Inorg. Chem.*, **20**, 4434 (1981); (c) M.G.B. Drew, J.M. Kisenyi, G.R. Willey, S.O. Wandiga. *J. Chem. Soc., Dalton Trans.*, 1717 (1984); (d) J.M. Kiseny, G.R. Willey, M.G.B. Drew. *J. Chem. Soc., Dalton Trans.*, 1073 (1985); (e) D.J. Williams, D. Vanderveer, R.L. Jones, D.S. Menaldino. *Inorg. Chim. Acta*, **165**, 173 (1989).
[24] S. Batsanow. *Inorg. Mater.*, **37**, 1031 (2001).
[25] A. Bondi. *J. Phys. Chem.*, **68**, 441 (1964).
[26] E.S. Raper, A.R.W. Jackson, D.J. Gardiner. *Inorg. Chim. Acta*, **84**, L1 (1984).
[27] H.W. Dias, M.R. Truter. *Acta Crystallogr.*, **17**, 937 (1964).
[28] U. Ohms, H. Guth, A. Kutoglu, C. Scheringer. *Acta Crystallogr.*, **B38**, 831 (1982).
[29] I. Haiduc, C. Silvestru. *Main Group Elements and their Compounds*, p. 355, Springer-Verlag, Berlin (1996).
[30] Oxford Diffraction. *CRYSALIS CCD and CRYSALIS RED, version p171.29.2*, Oxford Diffraction Ltd., Abingdon, Oxford, England (2006).
[31] CrysAlis RED, version 1.171.31.5; Oxford Diffraction Ltd. (release 28-08-2006 CrysAlis171.NET).
[32] G.M. Sheldrick. *Acta Crystallogr.*, **A46**, 467 (1990).
[33] G.M. Sheldrick. *SHELXL-97, Program for the Refinement of Crystal Structures*, University of Göttingen, Göttingen, Germany (1997).
[34] M.J. Frisch, G.W. Trucks, H.B. Schlegel, G.E. Scuseria, M.A. Robb, J.R. Cheeseman, J.A. Montgomery Jr, T. Vreven, K.N. Kudin, J.C. Burant, J.M. Millam, S.S. Iyengar, J. Tomasi, V. Barone, B. Mennucci, M. Cossi, G. Scalmani, N. Rega, G.A. Petersson, H. Nakatsuji, M. Hada, M. Ehara, K. Toyota, R. Fukuda, J. Hasegawa, M. Ishida, T. Nakajima, Y. Honda, O. Kitao, H. Nakai, M. Klene, X. Li, J.E. Knox, H.P. Hratchian, J.B. Cross, V. Bakken, C. Adamo, J. Jaramillo, R. Gomperts, R.E. Stratmann, O. Yazyev, A.J. Austin, R. Cammi, C. Pomelli, J.W. Ochterski, P.Y. Ayala, K. Morokuma, G.A. Voth, P. Salvador, J.J. Dannenberg, V.G. Zakrzewski, S. Dapprich, A.D. Daniels, M.C. Strain, O. Farkas, D.K. Malick, A.D. Rabuck, K. Raghavachari, J.B. Foresman, J.V. Ortiz, Q. Cui, A.G. Baboul, S. Clifford, J. Cioslowski, B.B. Stefanov, G. Liu, A. Liashenko, P. Piskorz, I. Komaromi, R.L. Martin, D.J. Fox, T. Keith, M.A. Al-Laham, C.Y. Peng, A. Nanayakkara, M. Challacombe, P.M.W. Gill, B. Johnson, W. Chen, M.W. Wong, C. Gonzalez, J.A. Pople, *GAUSSIAN-03, Revision C.02,* Gaussian, Inc., Wallingford, CT (2004).
[35] A.D. Becke. *J. Chem. Phys.*, **98**, 5648 (1993).
[36] C. Lee, W. Yang, R.G. Parr. *Phys. Rev.*, **B37**, 785 (1988).